DIGITAL SIMULATION OF INDUCTION START PERMANENT MAGNET SYNCHRONOUS MOTOR

S.SANKAR
Faculty in Dept. of EEE, SCSVMV University, Kanchipuram, Tamil Nadu, India.
Shankar_submanian@yahoo.co.in

Abstract: This paper model and simulates an Induction Start Permanent Magnet Synchronous (ISPMS) motor with asymmetry. The parameters like winding inductances and permanent magnet flux linkages are calculated directly from the geometry and winding layout of the machine using reluctance-mmf network. The model takes into account of many phenomena such as slot opening and the rotor movement, with a good compromise between calculation time and accuracy of results. Using the modified winding approach, the effect of salient pole rotor and stator winding mmf distribution on the inductances are closer to those obtained from finite element computation. The influence of slot opening on the air gap field distribution over the permanent magnet flux linkage has been studied. Finally, using these parameters the dynamic performance of an induction start permanent magnet synchronous motor is simulated and the results are shown to be in good agreement with the solution obtained by a conventional dq model.

Key words: *Induction start permanent magnet synchronous machine, Inductance, reluctance mmf network, permeance and flux linkages.*

1. Introduction

For many industrial applications, the development of Permanent Magnet (PM) machine becomes a powerful competitor for small rating drives due to their higher flux density and pullout torque as compared to the asynchronous machines such as, induction motor [1]-[4]. But, the cage winding is to develop good starting as well as accelerating torque. In particular, the Induction Start Permanent Magnet Synchronous motor combines the advantages of permanent magnet and cage winding. The size of motor is small and develops high inertia torque. Therefore, it can be used efficiently instead of conventional induction motor. For economical reason, the design of stator is similar to induction machine with three phase distributed winding in slots to produce the synchronously rotating quasi sinusoidal armature mmf wave form.

Usually, this type of motor has voltage source inverter circuit as integral part for variable speed applications and requires accurate prediction of motor parameters to obtain the desired the closed loop performance. Hence, a comprehensive model involves time varying parameters such as winding inductance and the PM induced flux linkage is needed. The conventional techniques, like, Finite Element Method and dq theory are used to find the parameter and also assess the performance of any AC machine. In [5]- [7] present a time stepping finite element analysis for ISPMS motors have cage bars with sufficient space for buried permanent magnets in the rotor. The cross sectional view of the ISPMS motor with cage bar is shown in Fig. 1. The time stepping finite element analysis offers detailed field calculations in regions with complex shapes. However, finding the solution for the set of nonlinear equations, for each rotor position gives rise to programming difficulties and requires powerful compute. In [8], the conventional dq model is used for analysis of an ISPMS motor. It is based on the assumption that the stator windings and air gap flux density are distributed sinusoidally. However, this assumption is far from reality under asymmetrical and/or faulty condition. Therefore, an effective modeling technique is required to combine the speed of the conventional dq model and the flexibility of FEM for studying the performance of ISPMS motors.

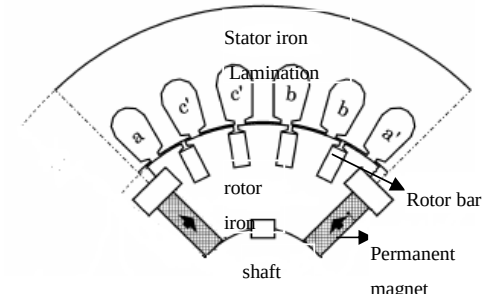

Fig. 1. Rotor Configuration.

The reluctance-mmf circuit has been widely used for modeling and simulation of induction motor . The main advantage of this model is that it is possible to predict transient and steady state performance of any machine with any type of winding distribution and air gap length. In the literature, it is considered to be less attractive for ISPMS motor. In this paper, the reluctance-mmf circuit model of the given motor is developed which includes stator and rotor teeth reluctances leads to analysis of small changes in designs but not gives reliable results in situation where completely new designs are being tried. A new comprehensive method for the calculation of parameters like, magnetic flux linkages, winding inductances are developed and using this performance of the ISPMS motor has been analyzed. The simulation results are verified with the conventional dq model results under symmetrical condition.

2. Mathematical Analysis

Consider an ISPMS motors having three balanced stator windings and rotor circuits with 'nr' identical bars and an end ring [8,9]. Let there be 'nm' pair of magnet bars buried in diametrically opposite in rotor create dq axis inductance and the same may be evaluated by using iterative technique under symmetry [10]. While consider an asymmetry and/or faulty condition, the calculation of parameters variation with respect to the rotor position is essential. The PM's are represented by constant current source i^m in parallel with recoil inductance L^{rc}. By applying Kirchhoff's and faradays law, the generalized equation of the proposed machine is written as

$$\left[V^s\right]=\left[R^s\right]\left[I^s\right]+\left[\frac{d\lambda^s}{dt}\right] \tag{1}$$

$$\left[V^r\right]=\left[R^r\right]\left[I^r\right]+\left[\frac{d\lambda^r}{dt}\right] \tag{2}$$

$$\lambda_a^s=\sum_{k=1}^{3}\sum_{l=1}^{3}L_{kl}^{ss}i_l^s+\sum_{k=1}^{3}\sum_{l=1}^{nr}L_{kl}^{sr}i_l^r\pm\sum_{k=1}^{3}\sum_{l=1}^{nm}L_{kl}^{rc}i_l^r \tag{3}$$

$$\lambda_{nl}^r=\sum_{k=1}^{nr}\sum_{l=1}^{3}L_{kl}^{rs}i_l^s+\sum_{k=1}^{nm}\sum_{l=1}^{3}L_{kl}^{rc}i_l^s\pm\left(\sum_{k=1}^{nr}\sum_{l=1}^{nr}L_{kl}^{rr}+\sum_{k=1}^{nm}\sum_{l=1}^{nm}L_{kl}^{rc}\right)i_l^r \tag{4}$$

Where,

R^s , R^r - A Diagonal matrix of stator and rotor resistance respectively.

L_{kl}^{ss} - Self and mutual inductance of stator coils.

$L_{kl}^{sr}=L_{kl}^{rsT}$ - Mutual inductance between stator coil and rotor bars nr.

L_{kl}^{rr} - Self and mutual inductance between rotor bars.

$i_{l,}^s i_{l,}^r$ - Stator coil and rotor bar current respectively.

$V_{,}^s V^r$ - Stator and rotor voltage respectively

$\lambda_{,}^s \lambda^r$ - Stator and rotor flux linkages respectively

The sign of the permanent magnet flux linkage depends on the orientation of the magnetic field produced by the magnets and coupled with stator windings are represented by an equivalent circuit as shown in fig. 2. Based on the geometrical information and winding layout of the machine given in the Appendix. I. the machine parameters with respect to position are calculated between any two windings k and l with a reasonable accuracy has been evaluated using magnetic coupled circuit model.

3. Reluctance-MMF Network

For easy understanding and reduce the computation timings of the machine, an ideal reluctance - mmf network is so helpful for analysis. The reluctance - mmf network is developed based on magnetic coupled circuit . The effect of saturation, fringing and leakage are neglected. The back iron parts in the stator and rotor have a large cross sectional area and nearly short length compared to the slot segment of stator and rotor. Therefore, the mmf drops in the stator and rotor yoke are much smaller than mmf drops in the teeth segments of stator and rotor. The stator winding comprises concentrated coils represented by equivalent stator teeth reluctance (R_{st}) in series with armature source mmf (F_{st}).

The PM is represented by a thevenien equivalent circuit consists of an mmf source (F_{pm}) in series with internal magnetic reluctance R_m [11]. Let R_{rt} is the reluctance of the rotor bar segment. To formulate the system of algebraic machine equations, only the number of slot per elementary pole pair needs to be modeled rather than simultaneous analysis of the complete circuit due to symmetry. The representative part of reluctance-mmf network is shown in Fig. 2. Then, the node potential equations of the network are given by

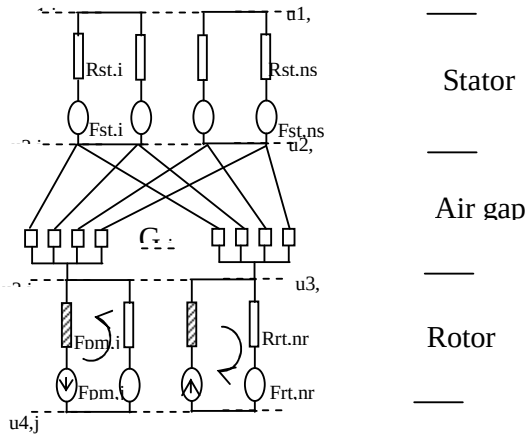

Fig. 2. The part of reluctance-mmf network

$$\begin{bmatrix} 0 & 0 & 0 & 0 \\ 0 & A_{22} & A_{23} & 0 \\ 0 & A_{32} & A_{33} & 0 \\ 0 & 0 & 0 & 0 \end{bmatrix} \begin{bmatrix} u_1 \\ u_2 \\ u_3 \\ u_4 \end{bmatrix} = \begin{bmatrix} -\sum_{i}^{ns} \phi_{si} \\ \phi_s \\ \phi_r \\ -\sum_{j}^{nr} \phi_{rj} \end{bmatrix} \quad (5)$$

$$u_2 = u_1 + R_{st}\phi_s + F_{st} \quad (6)$$

$$u_3 = u_4 + R_{rt}\phi_r + F_{rt} \quad (7)$$

Where,
u_1, u_2, u_3 and u_4 -the vectors of magnetic node potential.
Φ_{st} and Φ_{rt} -the vectors of stator and rotor teeth fluxes.
R_{st} and R_{rt} -the stator and rotor teeth reluctance matrices.
F_{st} and F_{rt} -the vectors of mmf source in the stator and rotor.
A_{22}, A_{23}, A_{32} and A_{33}-the node permeance matrices.

The reluctance-mmf network repeats the i_{th} tooth next to the first tooth. Therefore, equation (8) and (9) become necessary

$$\sum_{i}^{ns} \phi_{si} = 0; \quad (8)$$

$$\sum_{j}^{nr} \phi_{rj} = 0 \quad (9)$$

By substituting (8) and (9) in equation (5), then, u_1 and u_4 becomes zero. The node permeance matrix depends on stator slot, rotor slot and air gap permeance. The elements of node permeance matrices are given in the Appendix. II. It is calculated from magneto static Finite Element simulation package used is ANSOFT's Maxwell 2D model. The air-gap permeance is modeled with variable permeance for different stator-rotor tooth positions. Since, it depends on the relative position of rotor with respect to the stator. Usually, the stator pole arc is smaller than rotor pole arc. It means that the air gap permeance G_{ij} connecting i^{th} stator teeth with jth rotor segment are varies over an angular interval (θ). When θ is equal to zero (reference vale), the air gap flux path is maximum value i.e. the permeance function is maximum. When θ increases, rotor moves away from stator, the permeance value is reduced to zero as shown in Fig. 3.

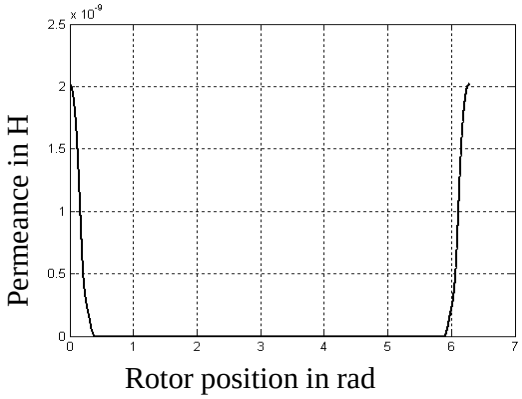

Fig. 3. Permeance Function

The stator mmf (F_{st}) and rotor mmf (F_{rt}) vectors in equation (6) and (7) are related to stator and rotor winding configuration and number of turns per coil. Then,

$$\int \frac{F_{st}(\varphi,\theta)}{G(\varphi,\theta)} d\varphi = \int \frac{N_s(\varphi,\theta)}{G(\varphi,\theta)} i_s d\varphi \quad (10)$$

$$\int \frac{F_{rt}(\varphi,\theta)}{G(\varphi,\theta)} d\varphi = \int \frac{N_r(\varphi,\theta)}{G(\varphi,\theta)} i_r d\varphi \quad (11)$$

Where, N_s and N_r is the magneto motive force transform matrix. φ is the stator reference frame. Using the modified winding function approach presented , F_{st} and F_{rt} are calculated for each coil at a certain rotor position. Which includes a periodic function of displacement about the air gap due to the saliency. It is well suited for studying the effect of machine under eccentricity.

4. Inductance Calculation

Once the magnetic coupled circuit is formed the inductance can be directly calculated by solving the above equations. Since there is no restriction concerning symmetry of stator winding, rotor bars, shape of PM and air gap length, this model may be applied in the study of asymmetrical effects and fault conditions. According to the magnetic coupled circuit theory, inductances of healthy machine as well as faulty machine can be calculated by substituting equation (4) and (5) into (2) and (3), and then rearranging parameters as follows

$$A_{22}N_s i_s + A_{23}N_r i_r = C\Phi s + A_{23}\ R_{rt}\Phi r \qquad (12)$$

$$A_{32}N_s i_s + A_{33}N_r i_r = D\Phi r + A_{32}\ R_{st}\Phi s \qquad (13)$$

Where,

$$C = (I_{ns\times ns} + A_{22}R_{st})$$

$$D = (I_{nr\times nr} + A_{33}R_{rt})$$

and by further simplification the following equations will be obtained.

$$N_s^T C^{-1}A_{22}N_s i_s + N_s^T C^{-1}A_{23}N_r i_r = N_s^T(\Phi_s + C^{-1}A_{23}\ R_{rt}\Phi_r) = \lambda_s \qquad (14)$$

$$N_r^T D^{-1}A_{32}N_s i_s + N_r^T D^{-1}A_{33}N_r i_r = N_r^T(\Phi_r + D^{-1}A_{32}\ R_{st}\Phi_s) = \lambda_r \qquad (15)$$

Comparing the equations (14) and (15) with the well known flux linkage equation (3) and (4) results in

$$L^{ss} = N_s^T C^{-1}A_{22}N_s \qquad (16)$$

$$L^{sr} = N_s^T C^{-1}A_{23}N_r \qquad (17)$$

$$L^{rs} = N_r^T D^{-1}A_{32}N_s \qquad (18)$$

$$L^{rr} = N_r^T D^{-1}A_{33}N_r \qquad (19)$$

It should be noted that due to the inclusion of stator and rotor teeth reluctances it is possible to study the effect of the magnetic property of different cores on machine inductances by this model. Therefore, this model is well suited for efficient design of ISPMS motors.

5. Simulation Results

The proposed algorithm is simulated using Matlab and SimuLink, Various simulation results are obtained with the specifications of the motor is given in the Appendix.1.

A. Computation of Inductance coefficient

In the simulation program an inductance matrix is needed to describe the connection between the each stator coils and rotor bars. The difference in permeability between rotor core and magnet results in self and mutual inductances are position dependent. Although, it is possible to calculate self inductance of each stator circuit at any position. Finally, the leakage inductances are calculated from the design data must be added to form the corresponding circuit self inductance. From the Fig. 4 one can observe that Self inductance of each stator circuit differs on the flux path with least reluctance path.

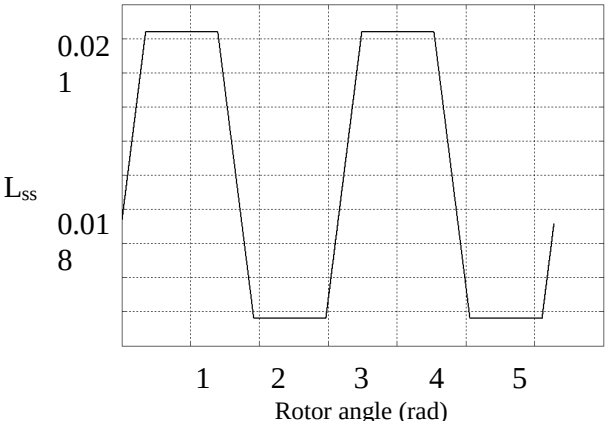

Fig. 4. Circuit self inductance

The mutual inductance between any two windings k and l in any electric machine can be computed by using flux linkage equation. There are two positions where the mutual inductance reaches its maximum as a result of the series connection of the member coils of the circuit. The effect of rotor skew, slot opening, static and dynamic eccentricity on mutual inductance has studied. Similar effect was experienced by the proposed machine also. The mutual inductance between stator phase and rotor loop as shown in fig. 5. In agreement with the finite element method.

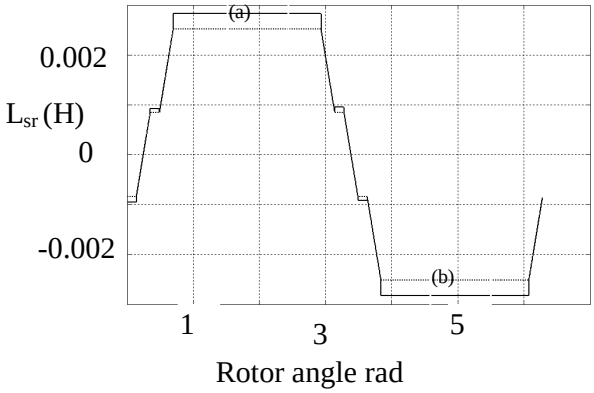

Fig. 5. Mutual inductance between stator phase and rotor loop (a) FEM method (b) proposed method

B. Flux linkage produced by PM

The flux linkage of the circuits produced by PM poles is another important issue in the simulation. Having the reluctance-mmf network, neglecting the internal magnetic reluctance and the assumption made previously, the total magnetic flux linkage is the sum of the flux linkages produced by the individual PM as

$$\lambda_{pm} = \pm \sum_{i=1}^{m} N_{r,i}^{2} G_{i,i} i_{r,i} \tag{20}$$

Where, m is the number of magnets in the circuit. The sign before λ_{pm} is determined by the manner in which the flux orientation of the magnet in the rotor circuit. Fig. 6. Shows the calculated flux linkage of each stator coil versus rotor positions where the flux linkage reaches its maximum magnitude which corresponds to the fact that the ISPMS motor has four PM poles.

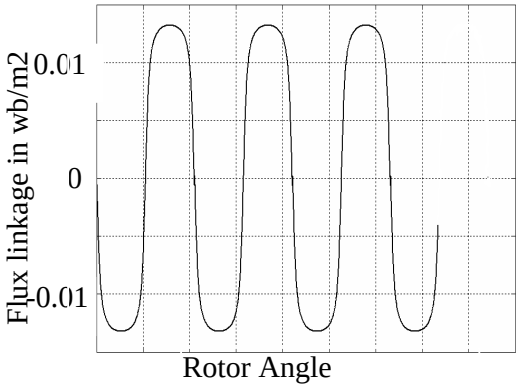

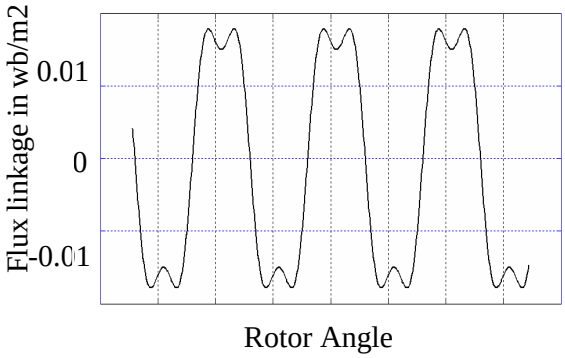

Fig. 6. Calculated Flux linkage produced by PM (a) Healthy condition (b) Including slot opening effect.

Comparison of plots 7(a) and 7(b) shows that the slot opening affects and degrades the shape of the flux linkages. In fact, the magnitude and frequency of ripple in plot 6(b) depend on slot opening width. The magnitude of ripple on these flux linkages introduces ripple in the torque production also.

C. Simulation of ISPMSM

A simulation study has been made to determine the performance of the ISPMS motor using the circuit equations (1) – (4), and the following torque and mechanical equations

$$T_e - T_m = J \frac{d\omega_m}{dt} \tag{21}$$

$$\omega_m = \frac{d\theta_m}{dt} \tag{22}$$

$$T_e = \sum_{i=1}^{ns} \sum_{j=1}^{nr} (u_{2i} - u_{3j})^2 \frac{dG_{ij}}{d\theta_m} \tag{23}$$

Where T_e is the electromechanical torque of machine, T_m is the load torque, θ_m is the mechanical angle, J is the inertia, ω_m is the mechanical speed and $dG_{ij}/d\theta_m$ is the derivative of air gap permeance with respect to the rotor position. Unlike the conventional synchronous motors, The ISPMS motor torque can be separated into three components. Namely, the permanent magnet creates a considerable braking torque during its asynchronous mode of operation as well as they help to synchronize with high inertia load. When the strength of the PM is too strong, the motor

may fail to synchronous because of the excessive pulsating torque component. The asynchronous torque developed by the cage winding aids to improve the line starting from standstill under transient period. The difference in permeability between the magnet and rotor core results in significant magnetic saliency and reluctance torque at steady state as shown in Fig. 7.

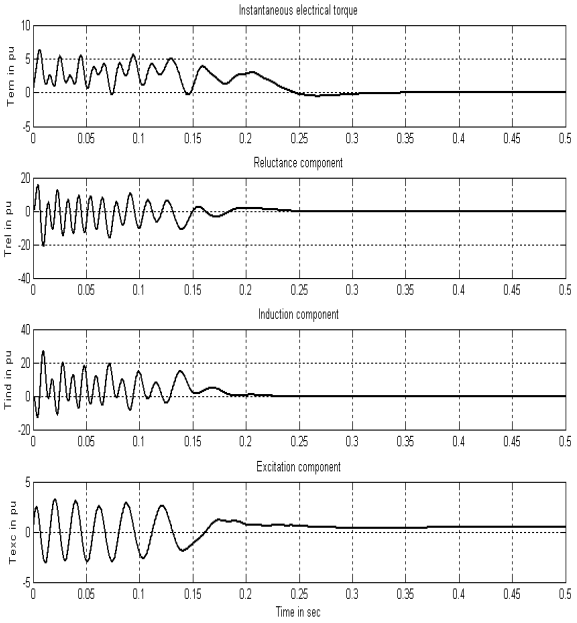

Fig. 7. Starting torque transients of ISPMS

For the purpose of comparison the model is first simulated using conventional dq model with sinusoidal voltage excitation and the results are shown in Fig. 8(a). In fig.8 (b). The same machine is simulated using the proposed method under the same conditions. Comparison of the two simulation traces shows very good correlation. The slight deviation appears to be caused by the harmonic effects created by the simulation of each separate winding circuit. The plots of motor speed from simulation are shown in fig. 9.

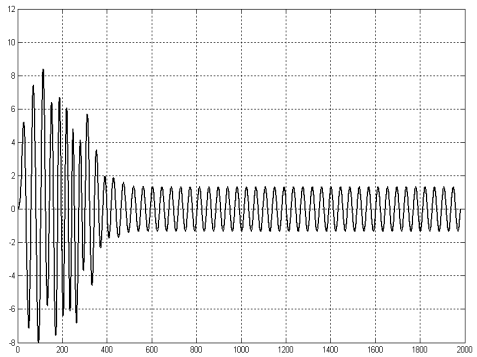

(a)

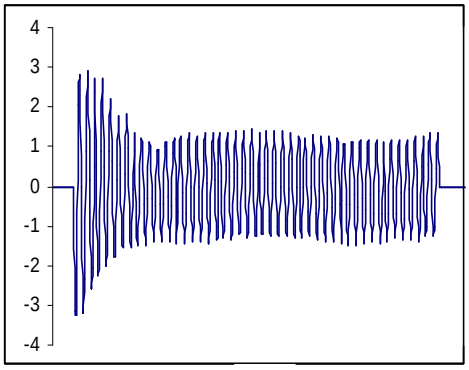

(b)

Fig. 8. Stator Phase current during start up in Ampere. (a) Conventional dq model (b) proposed model

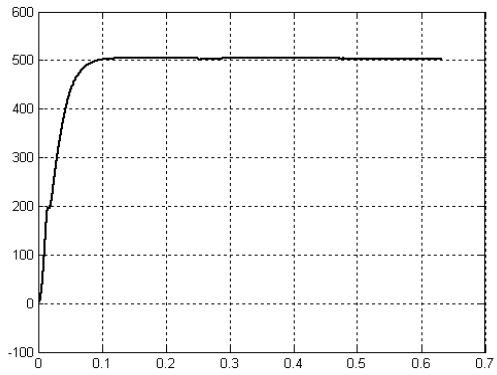

Fig. 9 Speed curves after start up

6. Conclusion

A new approach to induction start permanent magnet synchronous motor modeling has been developed based on the geometric and winding layout information. From the reluctance – mmf network, the self and mutual inductances and permanent magnet flux linkages were calculated on coil to coil basis. Simulation results have confirmed the validity of the model. Because the magnetic coupled circuit model takes into account arbitrary winding distribution, it should prove very useful for analyzing the slot opening effects also. It has also been shown that the results are consistent with the results of the conventional method for balanced operation.

References

1. K.J.Binns, and M.A.Jabbar:*High field self starting permanent magnet synchronous motor*, in proc. IEE., vol.128, pt.B. No.3, pp. 157-160, May 2004.

2. A.Levran, and E.Levi: *Design of poly phase motors with PM excitation*, IEEE Trans. On Magnetics, vol MAG-20, no.3, pp. 507–515, May 2006.

3. B.N.Chaudhari, S.K.Pillai and B.G.Fernandes:*Energy efficient line start permanent magnet synchronous motor*, Proc. Of IEEE Region ten conference-TENCON98, New Delhi, pp. 379–382, December 2004.

4. V.B.Honsinger: *The fields and parameters of interior type A.C. permanent magnet machines*, IEEE Trans. On Power Apparatus and Systems, vol PAS-101, no.3, pp. 867-875, 2005.

5. Kazumi Kurihara, and M.Azizur Rahman: *High efficiency line-start interior permanent magnet synchronous motors*, IEEE Trans. Industry Applications, vol. 40, no.3, pp. 789–796, May/June 2004.

6. S.L.Ho,H.L.Li,W.N.Fu, and H.C.Wong:*A Novel Approach to circuit- Field- Torque coupled time stepping finite element modeling of electric machines*, IEEE Trans. On Magnetics, vol 36, no.4, pp. 1886–1889, July 2004.

7. M.A.Jabbar, Zhejie Liu and Jing Dong: *Time stepping finite element analysis for the dynamic performance of a Permanent Magnet Synchronous Motor*, IEEE Trans. On Magnetics, vol 39, no.5, pp. 2621–2623, September 2003.

8. M.A.Rahman and A.M.Osheiba: *Performance of large line start permanent magnet synchronous motors*, *IEEE Trans. On Energy Conversion*, vol. 5, no.1, pp. 211-217, March 1999.

9. Xiaogang Luo, Yuefeng Liao, Hamid A.Toliyat, Ahmed EI- Antably and Thomas A,Lipo: *Multiple Coupled Circuit Modelling of Induction Machines*, IEEE Trans. Industry Applications, vol. 31, no.2, pp. 789–796, March/April 2004.

10. H.A.Toliyat and T.A.Lipo: *Transient analysis of cage IM under stator, rotor bar and end ring faults*, IEEE Trans. On Energy Conversion, vol. 10, no.2, pp. 241-247, June 2005.

11. Xiaogang Luo and Thomas.A.Lipo: *A synchronous/ Perm anent Magnet Hybrid AC Machine*, IEEE Trans. On Energy Conversion, vol. 15, no.2, pp. 203-210, June 2007.

APPENDIX

3ph, 4-poles, 220V, 4.7A, Y connected, single layer winding, 50hz, 0.6kw.		
Active axis length		75mm
Air gap length		0.7mm
Stack Factor		0.76mm
Stator	Slot Number	32
	Outer diameter	159mm
	Inner Diameter	80mm
	Slot Depth	18.4mm
	Slot Opening	3.3mm
	Slot bottom width	8.152mm
	Slot upper width	6.382mm
	Winding number	96 turns
Rotor	Slot Number	54
	Outer diameter	59.4mm
	Inner Diameter	40mm
	Slot Depth	9.85mm
	Inertia	0.00219kg.m^2